



RESEARCH REPOSITORY

This is the author's final version of the work, as accepted for publication following peer review but without the publisher's layout or pagination.

The definitive version is available at:

<https://doi.org/10.1158/1078-0432.CCR-15-1125>

Loi, S., Dushyanthen, S., Beavis, P.A., Salgado, R., Denkert, C., Savas, P., Combs, S., Rimm, D.L., Giltane, J.M., Estrada, M.V., Sanchez, V., Sanders, M.E., Cook, R.S., Pilkinton, M.A., Mallal, S.A., Wang, K., Miller, V. A., Stephens, P.J., Yelensky, R., Doimi, F.D., Gomez, H., Ryzhov, S.V., Darcy, P.K., Arteaga, C.L. and Balko, J.M. (2016) RAS/MAPK activation is associated with reduced Tumor-infiltrating lymphocytes in Triple-Negative Breast Cancer: Therapeutic Cooperation Between MEK and PD-1/PD-L1 Immune Checkpoint Inhibitors. *Clinical Cancer Research*, 22 (6). pp. 1499-1509.

<http://researchrepository.murdoch.edu.au/id/eprint/38797/>

Copyright: © 2015 American Association for Cancer Research
It is posted here for your personal use. No further distribution is permitted.



Published in final edited form as:

Clin Cancer Res. 2016 March 15; 22(6): 1499–1509. doi:10.1158/1078-0432.CCR-15-1125.

RAS/MAPK activation is associated with reduced tumor-infiltrating lymphocytes in triple-negative breast cancer: therapeutic cooperation between MEK and PD-1/PD-L1 immune checkpoint inhibitors

Sherene Loi^{1,2}, Sathana Dushyanthen¹, Paul A Beavis¹, Roberto Salgado³, Carsten Denkert⁴, Peter Savas¹, Susan Combs⁵, David L. Rimm⁵, Jennifer M. Giltneane^{6,9}, Monica V. Estrada⁹, Violeta Sánchez⁹, Melinda E. Sanders^{6,9}, Rebecca S. Cook^{8,9}, Mark A. Pilkinton⁷, Simon A. Mallal⁷, Kai Wang¹⁰, Vincent A. Miller¹⁰, Phil J. Stephens¹⁰, Roman Yelensky¹⁰, Franco D. Doimi¹¹, Henry Gómez¹¹, Sergey V. Ryzhov¹², Phillip K. Darcy^{1,2}, Carlos L. Arteaga^{7,8,9}, and Justin M. Balko^{7,9}

¹Peter MacCallum Cancer Centre, Melbourne, Victoria, Australia

²Sir Peter MacCallum Department of Oncology, University of Melbourne, Parkville, 3010, Australia

³Breast Cancer Translational Research Laboratory, Institute Jules Bordet, Brussels, Department of Pathology, GZA Antwerp, Belgium

⁴Charité University and German Cancer Consortium (DKTK), Berlin, Germany

⁵Departments of Pathology and Medicine, Yale University, New Haven, CT

⁶Department of Pathology, Microbiology & Immunology, Vanderbilt University, Nashville, TN 37232

⁷Department of Medicine, Vanderbilt University, Nashville, TN 37232

⁸Department of Cancer Biology, Vanderbilt University, Nashville, TN 37232

⁹Breast Cancer Program, Vanderbilt-Ingram Cancer Center; Nashville, TN 37232

¹⁰Foundation Medicine, Cambridge, MA 02142

¹¹Instituto Nacional de Enfermedades Neoplásicas (INEN), Lima, Perú

¹²Maine Medical Center Research Institute, Scarborough, ME, 04074

Abstract

Corresponding authors: Justin Balko, Vanderbilt University Medical Center, 2200 Pierce Ave, 777 PRB, Nashville, TN 37232-6307, justin.balko@vanderbilt.edu, Phone: (615) 875-8666, Fax: (615) 343343-7602, Sherene Loi, Peter MacCallum Cancer Centre, St Andrews Place, East Melbourne, Victoria, Australia 3002, sherene.loi@petermac.org, Phone: +61 3 9656 1111/3642, Fax: +61 3 9656 1411.

Conflicts of Interest: KW, PJS, RY, VAM, are paid employees and/or stockholders of Foundation Medicine. JMB, VS, and MES have filed provisionary patent on use of MHC-II to predict response to immunotherapy.

Purpose—Tumor-infiltrating lymphocytes (TILs) in the residual disease (RD) of triple-negative breast cancers (TNBCs) after neoadjuvant chemotherapy (NAC) are associated with improved survival, but insight into tumor cell-autonomous molecular pathways affecting these features are lacking.

Experimental Design—We analyzed TILs in the RD of clinically and molecularly characterized TNBCs after NAC and explored therapeutic strategies targeting combinations of MEK inhibitors with PD-1/PD-L1-targeted immunotherapy in mouse models of breast cancer.

Results—Presence of TILs in the RD was significantly associated with improved prognosis. Genetic or transcriptomic alterations in Ras/MAPK signaling were significantly correlated with lower TILs. MEK inhibition up-regulated cell-surface major histocompatibility complex (MHC) expression and PD-L1 in TNBC cells both *in vivo* and *in vitro*. Moreover, combined MEK and PDL-1/PD-1 inhibition enhanced anti-tumor immune responses in mouse models of breast cancer.

Conclusions—These data suggest the possibility that Ras/MAPK pathway activation promotes immune-evasion in TNBC, and support clinical trials combining MEK- and PD-L1-targeted therapies. Furthermore, Ras/MAPK activation and MHC expression may be predictive biomarkers of response to immune checkpoint inhibitors.

Keywords

MEK; immunotherapy; neoadjuvant chemotherapy

Introduction

Neoadjuvant chemotherapy (NAC) is used increasingly in patients with triple-negative breast cancer (TNBC), which does not express estrogen receptor, progesterone receptor or demonstrate human epidermal growth factor-2 (HER2) amplification. The purpose of NAC is to increase the patient's chances of undergoing breast-conserving surgery and to eliminate clinically silent micro-metastases. When employed, NAC results in a pathological complete response (pCR) in about 30% of TNBC patients. Achievement of a pCR predicts improved recurrence-free and overall survival (RFS and OS, respectively). Patients with residual disease (RD) in the breast or lymph nodes exhibit high rates of metastatic recurrence and an overall poor long term outcome(1).

The presence of tumor-infiltrating lymphocytes (TILs) in breast cancer specimens has been shown to be an important predictive and/or prognostic factor in TNBC. Retrospective analyses of several large clinical trials have demonstrated that high levels of TILs in the tumor are predictive of pCR to NAC, or increased disease-free survival and overall survival in randomized adjuvant studies(2,3). Furthermore, a recent retrospective analysis demonstrated that in NAC-treated TNBC patients with RD after chemotherapy (a known negative prognostic factor), the presence of TILs can further prognosticate patient outcome(4).

Aside from the obvious prognostic and predictive implications of these findings, the correlation of immune infiltrate with outcome in TNBC suggests that these patients may be candidates for immunotherapy. Recently, unprecedented and durable responses to

monoclonal antibodies (mAbs) interfering with immune checkpoints (PD-1, PD-L1, CTLA-4) have been observed in patients with advanced cancer(5–7). These responses have not been exclusive to putative ‘immunogenic’ tumor types, such as melanoma and renal cell carcinoma. There is emerging data demonstrating that other cancer types, such as TNBC, may have an immune component and thus, may benefit from immunotherapy. Furthermore, there are preclinical data suggesting that chemotherapy, which is more effective in TNBC and HER2+ disease, may work in part by engaging the immune system(8,9).

Despite the increasing evidence of the prognostic ability of TILs in TNBCs, little is known about what tumor cell-autonomous features may explain patient heterogeneity in TIL recruitment to the tumor microenvironment. Possible response factors include individual tumor mutation rates affecting neo-antigen presentation, presence of specific genomic alterations repressing or activating immune evasion, alterations and suppression of antigen-presenting pathways, and/or tumor microenvironment changes which create an immunosuppressive milieu. Specifically, there are no studies at present which have explored the contribution of tumor specific genomic and transcriptomic alterations that associate with TIL phenotypes. An improved understanding of these factors would permit combinatorial therapy to improve TIL recruitment, and the opportunity to determine if enhancing TIL recruitment can directly affect patient outcomes. To address this, we explored the presence of TILs within a molecularly and clinically characterized cohort of post-NAC TNBCs(10).

Herein, we present evidence that suggests that genomic or transcriptomic activation of the Ras/MAPK pathway is associated with suppressed TIL recruitment or retention. In multiple human and mouse datasets, activation of the Ras/MAPK pathway is linked to reduced levels of TILs as well as markers of T-cell immunity. Experimentally, we tested the effects of MEK inhibition on TNBC cell lines *in vitro* (human and mouse) and *in vivo* (mouse) and found that MEK inhibition upregulates MHC molecules and reduces immunosuppressive markers. Furthermore, the combination of MEK inhibition was synergistic with anti-PD1 antibodies in immunocompetent syngeneic mouse models of breast cancer. These data support clinical evaluation of this combination in TNBC patients in order to generate favorable and robust anti-tumor immunity.

Methods

Patient data

Clinical characteristics and molecular analysis of the patients were previously described(10). Briefly, the post-treatment data set consisted of 111 surgically resected tumor samples from patients with IHC and/or tNGS-confirmed TNBC, diagnosed and treated with NAC at the Instituto Nacional de Enfermedades Neoplásicas (Lima, Perú). The cohort was comprised predominately of node-positive patients. Clinical and pathologic data were retrieved from medical records under an institutionally approved protocol (INEN 10-018). In addition, 44 pre-treatment biopsies were available from matched patients. For most patients, NAC consisted of doxorubicin and cyclophosphamide every 3 weeks for 4 cycles. Approximately half of the patients received paclitaxel additionally (most commonly 12 weekly cycles).

TIL assessment

Determination of percentage of stromal lymphocytic infiltration (%TIL) in post-NAC and the TCGA BLBC primary tumors was performed as previously described(11) by two pathologists independently (RS and CD) using full face H&E sections. The average TILs value of the two measurements was then used for the survival analysis. The TILs variable was analyzed in using Cox regression survival models as a continuous variable. The Cox model was adjusted for tumor size, age, nodal status and residual disease tumor cellularity.

Immunohistochemistry

For HLA-A (Santa Cruz, sc-365485) staining, tissue microarrays were stained at 1:1300 dilution overnight at 4°C. Antigen retrieval was performed with a citrate buffer (pH 6) using a decloaking chamber (Biocare). The visualization system was Envision-Mouse using DAB chromogen and hematoxylin counterstaining. HLA-A positivity was scored manually, as average percent of positive tumor cell membranes in the TMA core/spot multiplied by the average intensity (0,1,2,3) for a final sample histoscore. For TMA analysis 1–3 independent cores/spots were averaged for each individual tumor.

For HLA-DR (immunofluorescence/AQUA), slides were deparaffinized with xylene and rehydrated with ethanol. Antigen retrieval was performed using citrate buffer (pH=6) or Tris EDTA buffer (pH=9), at a temperature of 97°C for 20 minutes. After blocking of endogenous peroxidase with methanol and hydroxyl peroxide, slides were pre-incubated with 0.3% bovine serum albumin in 0.1 mol/L of Tris-buffered saline for 30 minutes at room temperature. This was followed by incubation of the slides with the primary antibody (HLA-DR (TAL 1B5): sc-53319, mouse monoclonal antibody, Santa Cruz, Lot#: A0312; concentration 200 µg/ml) at a titer of 1 to 5000, and cytokeratin overnight at 4°C. Mouse EnVision reagent (DAKO, neat) and Alexa 546 conjugated goat anti-rabbit secondary antibody (Molecular Probes, Eugene, OR, 1 to 100) were used as secondary antibodies followed by Cy5-tyramide (Perker Elmer, Life Science, MA). DAPI staining containing 4'6-diamidino-2phenylindol was used to identify tissue nuclei. The staining conditions were optimized on tonsil whole tissue sections and breast cancer tissue micro arrays (TMAs) consisting of 40 tissue samples. The optimal titer for this antibody was chosen according to an expression range graph which allows objective assessment of the optimal dynamic range as well as signal to noise ratio of the marker of interest. The optimal dynamic range is calculated as the ratio between the top 10% to the lowest 10% AQUA scores for a given biomarker. PD-L1 immunofluorescence and AQUA was performed as previously described (12)

AQUA analysis

Protein expression levels were quantified using the AQUA method of quantitative immunofluorescence described previously(13). AQUA allows exact and objective measurement of fluorescence intensity within a defined tissue area, as well as within subcellular compartments. Briefly, a series of monochromatic high-resolution images were captured using an epifluorescent microscope platform and signal intensity of the target of interest was measured according to a previously described algorithm. For each TMA histospot, images were obtained for each fluorescence channel, DAPI (nuclei), Alexa 546

(cytokeratin), or Cy5 (target probe). In order to distinguish tumor from stroma and other parts, an epithelial tumor “mask” was created by dichotomizing the cytokeratin signal and target protein was quantified in the tumor (CK positive), the stroma (absence of CK positivity) or the total tissue area (all DAPI-positive cells) by dividing the target protein compartment pixel intensities by the area of the compartment within which they were measured (14).

Gene expression data analysis

Gene expression analysis for the MEK transcriptional signature on the post-NAC cohort was performed by nanoString as previously described(10). nanoString analysis for immune genes on mouse tumors was performed using the nanoString Pan-cancer immunology panel. Briefly, single cross sections of residual tumors following 14–17 days of treatment were used for RNA preparation and 50ng of total RNA >300nt was used for input into nCounter hybridizations. TCGA data were accessed through the cBio data portal(15), or through the TCGA data portal for processed RNA-SEQ data analysis. Basal-like status was determined from the TCGA RNA-SEQv2 level 3 data (accessed October 2, 2014) using the R package ‘genefu’. Two-hundred-six total basal-like cases were defined.

Cell lines

MMTV-neu cells were isolated from primary mammary tumor cells growing in transgenic FVB/N mice and passaged serially for >10 passages in DMEM/F12 media supplemented with 10% FBS, 20ng/mL EGF, 500ng/mL hydrocortisone, and 10ng/mL insulin to generate established cell lines. Presence of rat neu (western blot) in the cells is diagnostic for the authenticity of the cells and is performed on a regular basis. The C57BL/6 mouse breast carcinoma cell line AT-3 was obtained from Dr. Trina Stewart (Griffith University, Nathan, QLD, Australia) and were transduced to express chicken ovalbumin peptide as previously described (16). 4T1.2 cells were obtained from Prof. Robin Anderson (Peter MacCallum Cancer Centre). These cell lines were originally obtained from the ATCC, actively passaged for less than 6 months, and were authenticated using short tandem repeat profiling.

Mouse studies

For in vivo studies, 4T1.9 (Balb/c) or MMTV-neu (FVB) cells were injected in the #4 mammary gland (4T1.9: 5×10^4 cells; MMTV-neu: 1×10^6 cells) of syngeneic mice. AT3ova (C57Bl6 or RAG-deficient; 1×10^6 cells) were injected subcutaneously into the flank of syngeneic mice. Following the establishment of tumors ($50\text{--}250 \text{ mm}^3$), mice were treated with vehicle control (suspension agent or isotype IgG control), trametinib (1 mg/kg orally, once daily), selumetinib (50 mg/kg orally, twice daily), α -PD-1 (BioXcell clone RMP1-14, 200 μ g intraperitoneal, on days 0, 4, 8 and 12), or α -PD-L1 (Biolegend clone 10F.9G2, 100 μ g intraperitoneal, on days 0, 3 and 10). Tumor diameters were measured 2–3 times weekly with calipers and volume in mm^3 calculated using the formula ($\text{length}/2 \times \text{width}^2$). For pharmacodynamic analysis, mice were sacrificed 1 hr after the last dose of MEK inhibitor, and tumor lysates were analyzed by western blot or flow cytometry. At least six mice were used for each treatment arm in all experiments.

Flow cytometry

For *in vitro* analysis, cells were dissociated and collected with Accutase, washed twice with phosphate buffered saline and stained for 30 min at 4°C with fluorochrome-linked antibodies using DAPI as a viability control. Cells were rinsed three times after staining, prior to analysis. Stained cells were analyzed against appropriate fluorochrome-linked isotype controls on a 3-laser BD LSRII (BD Biosciences). For *in vivo* studies, after euthanizing mice, tumors were excised and digested using a mix of 1 mg/ml collagenase type IV (Sigma-Aldrich) and 0.02 mg/ml DNAase (Sigma-Aldrich). After a 45-minute digestion at 37°C, cells were twice passed through a 70 µm filter. Single cell suspensions were then analyzed by flow cytometry with 7AAD used to discriminate viable and dead cells. Expression of indicated markers on tumors was determined by flow cytometry by gating on CD45 negative and GFP positive cells (AT-3ovadim) or cherry positive cells (4T1ch9).

Immunoblotting

Immunoblotting was performed as previously described(17) using antibodies for p-ERK/12 (Cell Signaling,#9102), total ERK1/2 (Cell Signaling, #9101), GAPDH #(Abcam, Ab8245) or actin (Cell Signaling, #3700).

Lentiviral transduction of constitutively active MEK

MEK^{DD} and LACZ open reading frames were obtained from Addgene and cloned using Gateway recombination in pLX302 (18). The pLX302 vector was a gift from David Root (Addgene plasmid # 25896). MMTV-neu cells were transduced as previously described (10).

Statistical analysis

Statistics were performed as indicated using R or GraphPad Prism (GraphPad Software, San Diego, CA). A $p < 0.05$ was considered statistically significant for all studies.

Results

The post-NAC TIL phenotype predicts outcome in TNBC

High TILs in the residual tumor have been shown to associate with post-surgical outcome in NAC-treated TNBC patients(4). We wished to confirm this association in our own previously characterized post-NAC TNBC cohort(10,19). This cohort included 111 clinically-defined TNBCs including targeted next-generation sequencing (tNGS) on 74 tumors and nanoString gene expression analysis on 89 tumors. Importantly, this cohort included only patients with RD burden in the breast following NAC, as it is these patients most at risk for recurrence following definitive surgery. TILs were scored by expert pathologist review of hematoxylin and eosin (H&E)-stained whole tumor sections from pre-NAC (n=44) and post-NAC (n=92) specimens. The reviewers were blinded to all clinical and molecular data during scoring. Of the 44 matched samples, 5 post-NAC samples were residual disease in an associated lymph node, which could not be assessed for TILs. In paired samples (n=39), TILs tended to be reduced from the pre- to post-NAC specimen

($p=0.07$; Fig. 1A). No differences were noted in the change in TILs during NAC with respect to breast tumor molecular subtyping (Supplemental Fig. 1) or regimens containing a taxane (data not shown). Neither the pre-NAC nor the change in TILs was predictive of post-surgical relapse or survival, though the number of patients where pre-treatment data was available was comparably small (Supplemental Fig. 2). In contrast, however, the TIL population in the RD (post-NAC) was predictive of RFS and OS ($p=0.0005$ and $p=0.004$, respectively; Fig. 1B–C). A strong positive linear association of TILs in NAC-treated specimens was observed with RFS ($p=0.0001$, relative risk reduction of 3.4% for each 1% of TILs) and OS ($p=0.0016$; relative risk reduction of 2.8% for each % of TILs). In a multivariate analysis with stage, age, node status and tumor cellularity, TILs in the post-NAC disease remained a significant predictor of RFS and OS ($p=0.0008$ and $p=0.007$, respectively). Thus, our data are consistent in this cohort with what has been reported previously in a similar population(4).

Genomic or transcriptomic evidence of Ras/MAPK activation predicts a reduced TIL phenotype

To determine if TIL presence in residual TNBCs is associated with tumor-specific genomic alterations, we next tested whether actionable categories of genomic alterations (tNGS of 3,320 exons of 182 oncogenes and tumor suppressors plus 37 introns of 14 genes frequently rearranged in cancer(10)) were enriched with particular TIL phenotypes. Of the five previously defined categories(10) (cell cycle, Ras/MAPK, DNA repair, PI3K/mTOR, and growth factor receptors), we found an association of low TILs in the RD with the presence of potentially activating alterations in the Ras/MAPK pathway (amplifications in *KRAS*, *BRAF*, *RAF1* and truncations in *NF1*, 16% altered, $p=0.005$) (Fig. 1D). There was also a modest but significant association with activating cell cycle pathway alterations (*CCND1-3*, *CDK4*, *CDK6*, *CCNE1*, *RB*, *AURKA* and *CDKN2A*, 37% altered, $p=0.05$). No category of alterations was associated with TILs in pre-NAC specimens, though our power was limited as the sample size was smaller. In order to confirm the association of low TILs with alterations in the Ras/MAPK pathway in a more molecularly-defined subtype of breast cancer, we queried the basal-like primary breast cancers of the TCGA using *CD3E* mRNA expression as a surrogate for T-cell infiltration (Fig. 1E). Tumors with intermediate or low *CD3E* expression (suggesting reduced infiltrating T-cells) were enriched for Ras/MAPK pathway alterations ($p<0.0001$; Fig. 1F) including heterozygous loss of the negative regulator of ERK, *DUSP4*. Since it is possible that immunogenicity is a function of the degree of genome alteration (i.e. presence of neo-antigens(20,21)), we assessed the association of total number of alterations detected by tNGS with TILs, but did not detect a significant association in either the pre- or post-NAC sample set (Supplemental Fig.3). However, the lack of whole exome or genome sequencing coverage limits the interpretability of this analysis.

Since a transcriptional signature of MEK activation in the post-NAC specimen was previously shown to be predictive of RFS and OS in this cohort(10), we tested whether a high MEK transcriptional signature score(22) (assessed by nanoString analysis) correlated with reduced TILs within this cohort. We identified a significant linear inverse correlation between post-NAC TILs, but not pre-NAC TILs, with the MEK score ($r = -0.41$, $p=0.003$;

Fig. 2A–B). This finding was reproduced in a series of 201 samples from diverse genetically engineered mouse models (GEMM) of breast cancer(23), where *Cd3e* mRNA was significantly inversely associated with the mouse orthologous components of the MEK transcriptional signature ($r = -0.39$, $p < 0.0001$; Fig. 2C). An inverse association was also identified between the MEK score and stromal TILs, as scored by H&E review, in 206 basal-like tumors in the TCGA breast cancer data(Fig. 2D)(15,24). Although the anti-correlation was weaker in the primary basal-like breast cancer (BLBC) TCGA data, this discrepancy may be the result from enrichment of MEK-activation during chemotherapy observed in our post-NAC cohort(10,25,26). Confirming robustness of the TIL quantification, TILs were positively correlated with a number of prototypic T-cell markers, including *CD3E*, *CD4*, and *CD8A* mRNA.

The Ras/MAPK has been shown to suppress inflammatory responses mediated from cytokines such as $IFN\gamma$, which can potentiate antigen presentation via MHC-I and MHC-II as well as PD-L1 expression(27). Thus, we hypothesized that PD-L1, MHC-I and MHC-II expression in tumor cells is suppressed by Ras/MAPK activity, and this would be associated with reduced immune recognition and infiltration. We verified these associations in our own cohort, using dual-color AQUA for HLA-DR and PD-L1 expression (which is highly expressed in highly aggressive subtypes of breast cancer, Supplemental Fig. 4A and refs. (28–32)) in the tumor and stroma (each using cytokeratin masking), as well as standard IHC for HLA-A/MHC-I. In our own cohort, tumor-specific AQUA staining of HLA-DR or PD-L1 demonstrated tumor cell-specific membrane positivity in post-NAC TNBCs (Supplemental Fig.4B–C). PD-L1 expression was not uniformly changed pre- to post-NAC in matched patient specimens (Supplementary Fig. 4D–F). Next, we integrated TIL measurements and MEK signature scores, as well as AQUA/IHC for PD-L1, MHC-I, and MHC-II. We identified positive correlations among MHC-I, MHC-II, and PD-L1, and anti-correlations between these markers and MEK transcriptional activity (Fig. 2E). Together, these data suggest that there is a negative association between MEK activity and active antigen presentation (MHC-I and II expression) that appears to be coupled to simultaneous PD-L1 expression which likely suppresses active antitumor immunity.

MEK inhibition upregulates $IFN\gamma$ -mediated MHC-I/II molecules and PD-L1 expression in mouse-derived breast cancer cell lines in vitro and in vivo

We next investigated if MEK inhibition could favorably affect the level of relevant immune molecules (including MHC-I, MHC-II, and PD-L1). To address this, we utilized mouse mammary tumor-derived cell lines, since they could be readily transplanted in immunocompetent syngeneic hosts to explore *in vivo* interplay with the immune system. Using cultured AT3ova and 4T1.9 mouse TNBC cell lines, we found that MEK inhibition with trametinib potentiated the effect of interferon-gamma ($IFN\gamma$) on expression of MHC-I (H2Kd and H2Dd), MHC-II (IA-IE) and Pd-l1 (Fig. 3A–B). $IFN\gamma$ is secreted from activated CTLs and can induce MHC-I and MHC-II expression in target cells to promote immune-mediated cytotoxicity. These findings were confirmed *in vivo*, following orthotopic injection of the established cell line into syngeneic WT mice and oral trametinib treatment (Fig. 3C–F). Thus, MEK activity can suppress $IFN\gamma$ -induced antigen presentation and thus may be a mechanism whereby Ras/MAPK activation supports immune evasion. In both AT3ova and

4T1.9 models, MEK inhibition suppressed the growth of tumors *in vivo* (Fig. 3C–D), although this cannot be entirely explained by immune-interaction, as trametinib also suppressed proliferation to some degree *in vitro* (Supplemental Fig. 5). To verify that genetic activation of the Ras/MAPK pathway could suppress MHC expression, we transduced MMTV-neu cells with pLX302-LACZ-V5 and pLX302-MEK^{DD}-V5, a constitutively-active MEK mutant. MEK^{DD} expression induced ERK activation (Fig. 3G), as expected, and suppressed IFN γ -mediated PD-L1 and MHC-II expression (Fig. 3H).

Combined MEK inhibition with immune antibodies targeting PD-1/PD-L1 in murine syngeneic tumor models are associated with increased efficacy

Because IFN γ -induced PD-L1 was also potentiated by MEK inhibition, we hypothesized that MEK inhibition may prime tumor cells for immune-mediated rejection by unleashing antigen presentation, but fail to fully respond because PD-L1 is coordinately upregulated. Thus, we tested whether combined MEK and PD-1 or PD-L1 inhibition would have combinatorial activity *in vivo*.

Two syngeneic tumor models were used (AT3ova [TNBC] and MMTV-neu [HER2+]). For the orthotopic AT3ova TNBC model, concomitant trametinib and α -PD1 was more effective than either single agent or vehicle control (Fig 4A). When the same experiment was performed in RAG-deficient mice, which lack functional T and B cells, the effect of MEK inhibition was diminished, while the effect of PD-1 antibody was abrogated (Fig. 4B). These data indicate at least part of the therapeutic efficacy of MEK inhibition in this model is immune-mediated and are consistent with the partial effect observed with MEK inhibition on proliferation alone *in vitro*. For the MMTV-neu model, we utilized 2 derivative cell lines: MMTV-neu stably transduced with pLX302-LACZ-V5 and pLX302-MEK^{DD}-V5, a constitutively-active MEK mutant. The control (LACZ) tumor line was moderately sensitive to α -PD-L1 (complete regression in 1/8 tumors), while the addition of a MEK inhibitor (selumetinib) to α -PD-L1 caused complete regression in 5/6 tumors (Fig. 4C and Supplemental Fig. 6). We utilized the interaction effect in a 2-way ANOVA using the log-transformed tumor volumes at 14d to assess synergy between the MEK inhibition and α -PD-L1 therapy. There was a significant interaction effect ($p=0.024$) in the LACZ (control model), suggesting synergy between these agents. In contrast, in the MMTV-neu/MEK^{DD} model, α -PD-L1 was not effective, except in combination with MEKi. In this model, the combination was more effective than either single agent alone (Fig. 4D). The interaction effect was not significant in the MEK^{DD} model, presumably because little effect was seen with anti-PD-L1 or selumetinib alone. In both the MMTV-neu and AT3ova models, pharmacodynamic efficacy of selumetinib or trametinib (inhibition of p-ERK1/2) was observed in tumors (Supplemental Fig. 7). Furthermore, mRNA expression analysis (nanoString mouse Pan-Cancer-Immune panel) of the treated tumors demonstrated that genetic activation of MEK suppressed antigen presentation and processing genes, while treatment with anti-PD-L1 (LacZ) or co-treatment of selumetinib and anti-PD-L1 (MEK^{DD}) increased the expression of these genes (Fig. 4E). Gene expression of *PD-L1* (*Cd274*) and *Cd3e* followed similar patterns (Fig. 4F), demonstrating a role for genetic activation of MEK (and pharmacologic inhibition) in modulation of T-cell infiltration into mammary tumors. These data suggest that MEK activation can promote resistance to PD-L1 targeted therapy

and also support clinical trials testing the combination in patients with TNBC or HER2+ breast cancer, particularly in cases with reduced TILs. Importantly, similar results were achieved with different MEK inhibitors (trametinib or selumetinib) and PD-1 pathway inhibitors (α -PD-L1 or α -PD-1) strengthening conclusions based on pathway-specific effects of these agents.

Discussion

There is increasing evidence that TILs are a positive prognostic biomarker in TNBC and that the quantity of TILs present is important- the more present, the better the survival. Furthermore, the field is becoming increasingly aware that immunomodulatory therapies may be effective in a wider variety of human malignancies than previously thought. However, thus far there have been little data available on tumor-autonomous molecular features that may be causal in the TIL/immunoregulatory phenotype. With the advent of effective immunotherapies, strategies targeted at high and low TIL phenotypes may emerge. Herein, we have characterized TIL phenotypes in a unique cohort of TNBCs after NAC, which, by nature as a clinical group, represent a population of patients with poor outcome. Importantly, in this subset of patients, the standard of care is observation even though the rate of subsequent metastatic recurrence is very high. Since patients at this point in care likely harbor clinically silent micro-metastases, the immediate post-operative period may represent an optimal time for the delivery of immunotherapy.

We demonstrate that Ras/MAPK activity can suppress expression of MHC-I and MHC-II, both intrinsically and those induced by IFN γ . These data led to the hypothesis that tumor cells can circumvent antigen presentation pathways by activating the MAPK pathway and that therapeutic inhibition of MEK can unleash these signals. These results are consistent with those published in melanoma(27,33), although the mechanism has not yet been elucidated. Thus, we hypothesize that combinatorial inhibition of both MEK and PD-L1 should yield improved responses to immunotherapy by down regulating immunosuppressive factors and up-regulating MHC-I/II to prime and synergize in response to T-cell checkpoint blockade resulting in functional anti-tumor immunity and increased lymphocytic infiltration.

While immune checkpoint inhibitors have pronounced activity in tumors with high mutational load (i.e. melanoma(34), lung cancer, and microsatellite-instable colorectal cancer(35)), tumor types with lower mutational burden have been shown to have modest but significant activity. Importantly, immune checkpoint inhibitors (specifically those antibodies targeting PD-1) have recently been shown to have efficacy in TNBC(36,37) which tend to have reduced mutational loads(24). Therefore, since the response rates to single agent therapy were relatively low (10–20%), strategies to enhance response rates through patient selection and combinations of existing therapies represent an obvious next hurdle to bringing immune therapies to breast cancer patients. In our study, we found that approximately 15% of TNBCs were Ras/MAPK altered at the genomic level, while a greater percentage had evidence of MEK activation at the transcriptomic level. Our data also suggest that activation of the Ras/MAPK pathway and MHC-I/II expression may be useful biomarkers to explore in future clinical trials of PD-1/PD-L1 inhibitors in TNBC. Based on these results, we propose clinical trials combining MEK inhibitors with antibodies targeting

the PD-1/PD-L1 axis to determine whether this combination results in more potent anti-tumor immune responses in patients.

Supplementary Material

Refer to Web version on PubMed Central for supplementary material.

Acknowledgements

JMB was supported by the Inflammatory Breast Cancer (IBC) Network Foundation, Susan G. Komen for the Cure Foundation CCR14299052, the NIH/NCI (1K99CA181491), the Breast Cancer Specialized Program of Research Excellence (SPORE) P50 CA098131, Vanderbilt-Ingram Cancer Center Support Grant P30 CA68485. CLA is also supported by Susan G. Komen for the Cure Foundation Grant SAC100013. SL, DS, PAB, PS and PKD are supported by the National Breast Cancer Foundation of Australia. SL is also supported by Cancer Council Victoria, Australia.

References

- Liedtke C, Mazouni C, Hess KR, Andre F, Tordai A, Mejia JA, et al. Response to neoadjuvant therapy and long-term survival in patients with triple-negative breast cancer. *J Clin Oncol.* 2008; 26(8):1275–1281. [PubMed: 18250347]
- Adams S, Gray RJ, Demaria S, Goldstein L, Perez EA, Shulman LN, et al. Prognostic Value of Tumor-Infiltrating Lymphocytes in Triple-Negative Breast Cancers From Two Phase III Randomized Adjuvant Breast Cancer Trials: ECOG 2197 and ECOG 1199. *J Clin Oncol.* 2014
- Loi S, Michiels S, Salgado R, Sirtaine N, Jose V, Fumagalli D, et al. Tumor infiltrating lymphocytes are prognostic in triple negative breast cancer and predictive for trastuzumab benefit in early breast cancer: results from the FinHER trial. *Ann Oncol.* 2014; 25(8):1544–1550. [PubMed: 24608200]
- Dieci MV, Criscitiello C, Goubar A, Viale G, Conte P, Guarneri V, et al. Prognostic value of tumor-infiltrating lymphocytes on residual disease after primary chemotherapy for triple-negative breast cancer: a retrospective multicenter study. *Ann Oncol.* 2014; 25(3):611–618. [PubMed: 24401929]
- Brahmer JR, Tykodi SS, Chow LQ, Hwu WJ, Topalian SL, Hwu P, et al. Safety and activity of anti-PD-L1 antibody in patients with advanced cancer. *N Engl J Med.* 2012; 366(26):2455–2465. [PubMed: 22658128]
- Topalian SL, Hodi FS, Brahmer JR, Gettinger SN, Smith DC, McDermott DF, et al. Safety, activity, and immune correlates of anti-PD-1 antibody in cancer. *N Engl J Med.* 2012; 366(26):2443–2454. [PubMed: 22658127]
- Robert C, Thomas L, Bondarenko I, O'Day S, Weber J, Garbe C, et al. Ipilimumab plus dacarbazine for previously untreated metastatic melanoma. *N Engl J Med.* 2011; 364(26):2517–2526. [PubMed: 21639810]
- Sistigu A, Yamazaki T, Vacchelli E, Chaba K, Enot DP, Adam J, et al. Cancer cell-autonomous contribution of type I interferon signaling to the efficacy of chemotherapy. *Nat Med.* 2014; 20(11):1301–1309. [PubMed: 25344738]
- Loi S, Pommey S, Haibe-Kains B, Beavis PA, Darcy PK, Smyth MJ, et al. CD73 promotes anthracycline resistance and poor prognosis in triple negative breast cancer. *Proc Natl Acad Sci U S A.* 2013; 110(27):11091–11096. [PubMed: 23776241]
- Balko JM, Giltane JM, Wang K, Schwarz LJ, Young CD, Cook RS, et al. Molecular profiling of the residual disease of triple-negative breast cancers after neoadjuvant chemotherapy identifies actionable therapeutic targets. *Cancer Discov.* 2014; 4(2):232–245. [PubMed: 24356096]
- Salgado R, Denkert C, Demaria S, Sirtaine N, Klauschen F, Pruneri G, et al. The evaluation of tumor-infiltrating lymphocytes (TILs) in breast cancer: recommendations by an International TILs Working Group 2014. *Ann Oncol.* 2015; 26(2):259–271. [PubMed: 25214542]
- Wimberly H, Brown JR, Schalper K, Haack H, Silver MR, Nixon C, et al. PD-L1 Expression Correlates with Tumor-Infiltrating Lymphocytes and Response to Neoadjuvant Chemotherapy in Breast Cancer. *Cancer Immunol Res.* 2014

13. Camp RL, Chung GG, Rimm DL. Automated subcellular localization and quantification of protein expression in tissue microarrays. *Nat Med.* 2002; 8(11):1323–1327. [PubMed: 12389040]
14. Brown JR, Wimberly H, Lannin DR, Nixon C, Rimm DL, Bossuyt V. Multiplexed quantitative analysis of CD3, CD8, and CD20 predicts response to neoadjuvant chemotherapy in breast cancer. *Clin Cancer Res.* 2014; 20(23):5995–6005. [PubMed: 25255793]
15. Cerami E, Gao J, Dogrusoz U, Gross BE, Sumer SO, Aksoy BA, et al. The cBio cancer genomics portal: an open platform for exploring multidimensional cancer genomics data. *Cancer Discov.* 2012; 2(5):401–404. [PubMed: 22588877]
16. Mattarollo SR, Loi S, Duret H, Ma Y, Zitvogel L, Smyth MJ. Pivotal role of innate and adaptive immunity in anthracycline chemotherapy of established tumors. *Cancer Res.* 2011; 71(14):4809–4820. [PubMed: 21646474]
17. Balko JM, Jones BR, Coakley VL, Black EP. MEK and EGFR inhibition demonstrate synergistic activity in EGFR-dependent NSCLC. *Cancer Biol Ther.* 2009; 8(6):522–530. [PubMed: 19305165]
18. Yang X, Boehm JS, Salehi-Ashtiani K, Hao T, Shen Y, Lubonja R, et al. A public genome-scale lentiviral expression library of human ORFs. *Nat Methods.* 2011; 8(8):659–661. [PubMed: 21706014]
19. Loi S, Sirtaine N, Piette F, Salgado R, Viale G, Van Eenoo F, et al. Prognostic and predictive value of tumor-infiltrating lymphocytes in a phase III randomized adjuvant breast cancer trial in node-positive breast cancer comparing the addition of docetaxel to doxorubicin with doxorubicin-based chemotherapy: BIG 02-98. *J Clin Oncol.* 2013; 31(7):860–867. [PubMed: 23341518]
20. Rooney MS, Shukla SA, Wu CJ, Getz G, Hacohen N. Molecular and genetic properties of tumors associated with local immune cytolytic activity. *Cell.* 2015; 160(1–2):48–61. [PubMed: 25594174]
21. Kreiter S, Vormehr M, van de Roemer N, Diken M, Lower M, Diekmann J, et al. Mutant MHC class II epitopes drive therapeutic immune responses to cancer. *Nature.* 2015; 520(7549):692–696. [PubMed: 25901682]
22. Pratilas CA, Taylor BS, Ye Q, Viale A, Sander C, Solit DB, et al. (V600E)BRAF is associated with disabled feedback inhibition of RAF-MEK signaling and elevated transcriptional output of the pathway. *Proc Natl Acad Sci U S A.* 2009; 106(11):4519–4524. [PubMed: 19251651]
23. Herschkowitz JI, Simin K, Weigman VJ, Mikaelian I, Usary J, Hu Z, et al. Identification of conserved gene expression features between murine mammary carcinoma models and human breast tumors. *Genome Biol.* 2007; 8(5):R76. [PubMed: 17493263]
24. TCGA. Comprehensive molecular portraits of human breast tumours. *Nature.* 2012; 490(7418):61–70. [PubMed: 23000897]
25. Balko JM, Cook RS, Vaught DB, Kuba MG, Miller TW, Bholra NE, et al. Profiling of residual breast cancers after neoadjuvant chemotherapy identifies DUSP4 deficiency as a mechanism of drug resistance. *Nat Med.* 2012; 18(7):1052–1059. [PubMed: 22683778]
26. Balko JM, Schwarz LJ, Bholra NE, Kurupi R, Owens P, Miller TW, et al. Activation of MAPK pathways due to DUSP4 loss promotes cancer stem cell-like phenotypes in basal-like breast cancer. *Cancer Res.* 2013
27. Hu-Lieskovan S, Mok S, Homet Moreno B, Tsoi J, Robert L, Goedert L, et al. Improved antitumor activity of immunotherapy with BRAF and MEK inhibitors in BRAF(V600E) melanoma. *Sci Transl Med.* 2015; 7(279):279ra41.
28. Ghebeh H, Mohammed S, Al-Omair A, Qattan A, Lehe C, Al-Qudaihi G, et al. The B7-H1 (PD-L1) T lymphocyte-inhibitory molecule is expressed in breast cancer patients with infiltrating ductal carcinoma: correlation with important high-risk prognostic factors. *Neoplasia.* 2006; 8(3): 190–198. [PubMed: 16611412]
29. Mittendorf EA, Philips AV, Meric-Bernstam F, Qiao N, Wu Y, Harrington S, et al. PD-L1 expression in triple-negative breast cancer. *Cancer Immunol Res.* 2014; 2(4):361–370. [PubMed: 24764583]
30. Muenst S, Schaerli AR, Gao F, Daster S, Trella E, Drosner RA, et al. Expression of programmed death ligand 1 (PD-L1) is associated with poor prognosis in human breast cancer. *Breast Cancer Res Treat.* 2014; 146(1):15–24. [PubMed: 24842267]

31. Muenst S, Soysal SD, Gao F, Obermann EC, Oertli D, Gillanders WE. The presence of programmed death 1 (PD-1)-positive tumor-infiltrating lymphocytes is associated with poor prognosis in human breast cancer. *Breast Cancer Res Treat.* 2013; 139(3):667–676. [PubMed: 23756627]
32. Soliman H, Khalil F, Antonia S. PD-L1 expression is increased in a subset of basal type breast cancer cells. *PLoS One.* 2014; 9(2):e88557. [PubMed: 24551119]
33. Kakavand H, Wilmott JS, Menzies AM, Vilain R, Haydu LE, Yearley JH, et al. PD-L1 expression and tumor-infiltrating lymphocytes define different subsets of MAPK inhibitor treated melanoma patients. *Clin Cancer Res.* 2015
34. Larkin J, Chiarion-Sileni V, Gonzalez R, Grob JJ, Cowey CL, Lao CD, et al. Combined Nivolumab and Ipilimumab or Monotherapy in Untreated Melanoma. *N Engl J Med.* 2015; 373(1): 23–34. [PubMed: 26027431]
35. Le DT, Uram JN, Wang H, Bartlett BR, Kemberling H, Eyring AD, et al. PD-1 Blockade in Tumors with Mismatch-Repair Deficiency. *N Engl J Med.* 2015; 372(26):2509–2520. [PubMed: 26028255]
36. Emens, LA.; Braiteh, FS.; Cassier, P., et al. Inhibition of PD-L1 by MPDL3280A leads to clinical activity in patients with metastatic triple-negative breast cancer (TNBC). Presented at the American Association for Cancer Research Annual Meeting; Philadelphia. Abstract 2859 2015.
37. Nanda R, Chow LQ, Dees EC, Berger R, Gupta S, Geva R, et al. A phase Ib study of pembrolizumab (MK-3475) in patients with advanced triple-negative breast cancer [abstract]. *Cancer Res.* 2015; 75(9 Suppl) Abstract nr S1-09.
38. Benjamini Y, Hochberg Y. Controlling the False Discovery Rate: A Practical and Powerful Approach to Multiple Testing. *Journal of the Royal Statistical Society Series B (Methodological).* 1995; 57(1):289–300.

Statement of translational relevance

The presence of tumor-infiltrating lymphocytes is an important prognostic factor in triple-negative breast cancer, but the molecular source of heterogeneity in host anti-tumor immunity is unknown. Our data shed preliminary insight into the tumor cell-autonomous pathways that may promote host anti-tumor immune evasion, and as a result, suggest combinations of molecularly targeted agents to overcome these features.

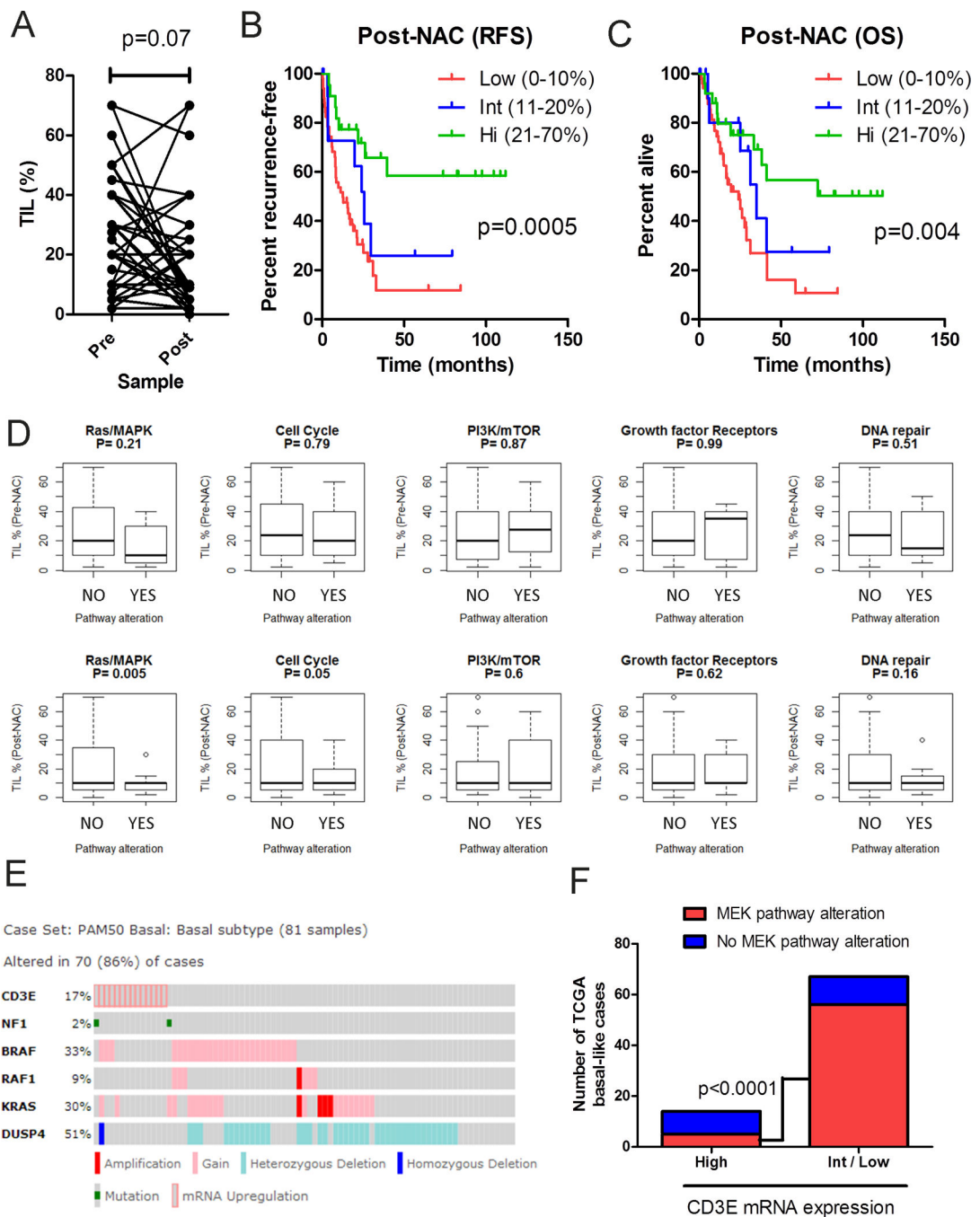


Figure 1. Low levels of tumor-infiltrating lymphocytes are associated with reduced survival and genomic alterations in the Ras/MAPK pathway

A) TILs were scored in 39 matched pairs of TNBC before (diagnostic biopsy) and after (surgical specimen). Change in the percent infiltrating lymphocytes was compared by a paired 2-way student’s t-test. B) Kaplan-Meier analysis of RFS or OS (C) after surgical resection according to post-NAC TIL quantile (tertiles). P-value represents the log-rank trend test. (D) Association of TILs in the diagnostic (Pre-NAC; upper panels) and surgical (post-NAC; lower panels) with genomic alterations detected by tNGS. Alterations were categorized as previously described(10). P-value represents the result of a student’s t-test.

E) and F) Mutual exclusivity of Ras/MAPK pathway alterations in the TCGA basal-like breast cancer dataset (15,24) using *CD3E* mRNA expression as a marker of T-cell infiltrate. P-value represents the result of a Fisher's exact test.

Author Manuscript

Author Manuscript

Author Manuscript

Author Manuscript

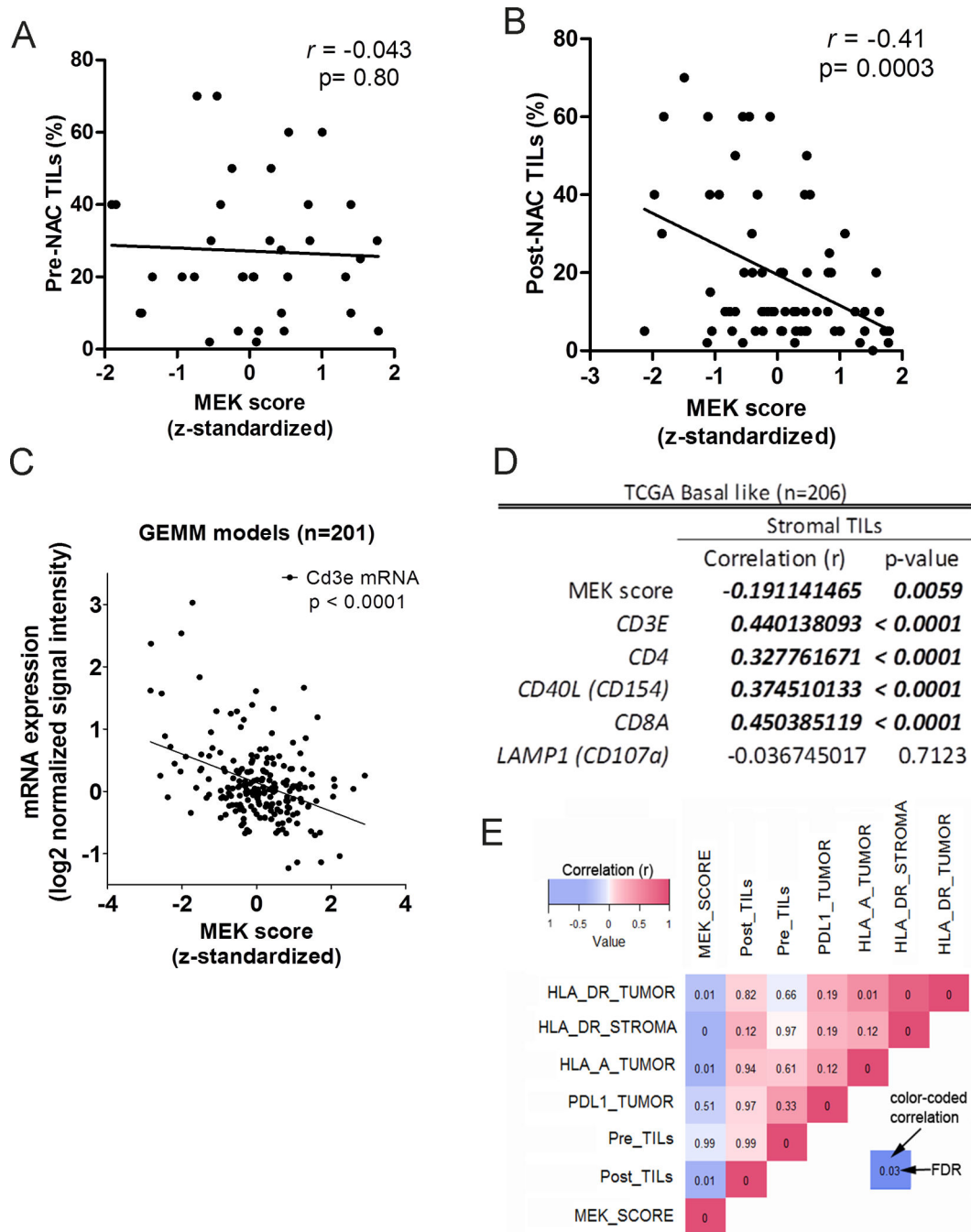


Figure 2. Transcriptional activation of the Ras/MAPK pathway predicts low immune infiltrate in post-NAC TNBC

A) Linear association of the z-standardized MEK transcriptional score (assessed from post-NAC tissues) compared to the TIL score prior to (A) or following (B) NAC. C) Linear association of the z-standardized MEK transcriptional score (orthologous mouse genes were identified using the HomoloGene database, www.ncbi.nlm.nih.gov) compared to *Cd3e* mRNA expression in 201 samples from diverse GEMMs. D) Table of linear associations of stromal TILs with the z-standardized MEK transcriptional score or mRNA expression of selected T-lymphocytic markers in 206 RNA-SEQ samples from primary basal-like breast

cancer samples in the TCGA. E) Heatmap correlation matrix of association of TILs with MEK transcriptional signature and IHC markers in post-NAC TNBC. Color represents the correlation coefficient, while the value represents the Benjamini-Hochberg(38) false discovery rate (multiple-comparisons-adjusted p-value).

Author Manuscript

Author Manuscript

Author Manuscript

Author Manuscript

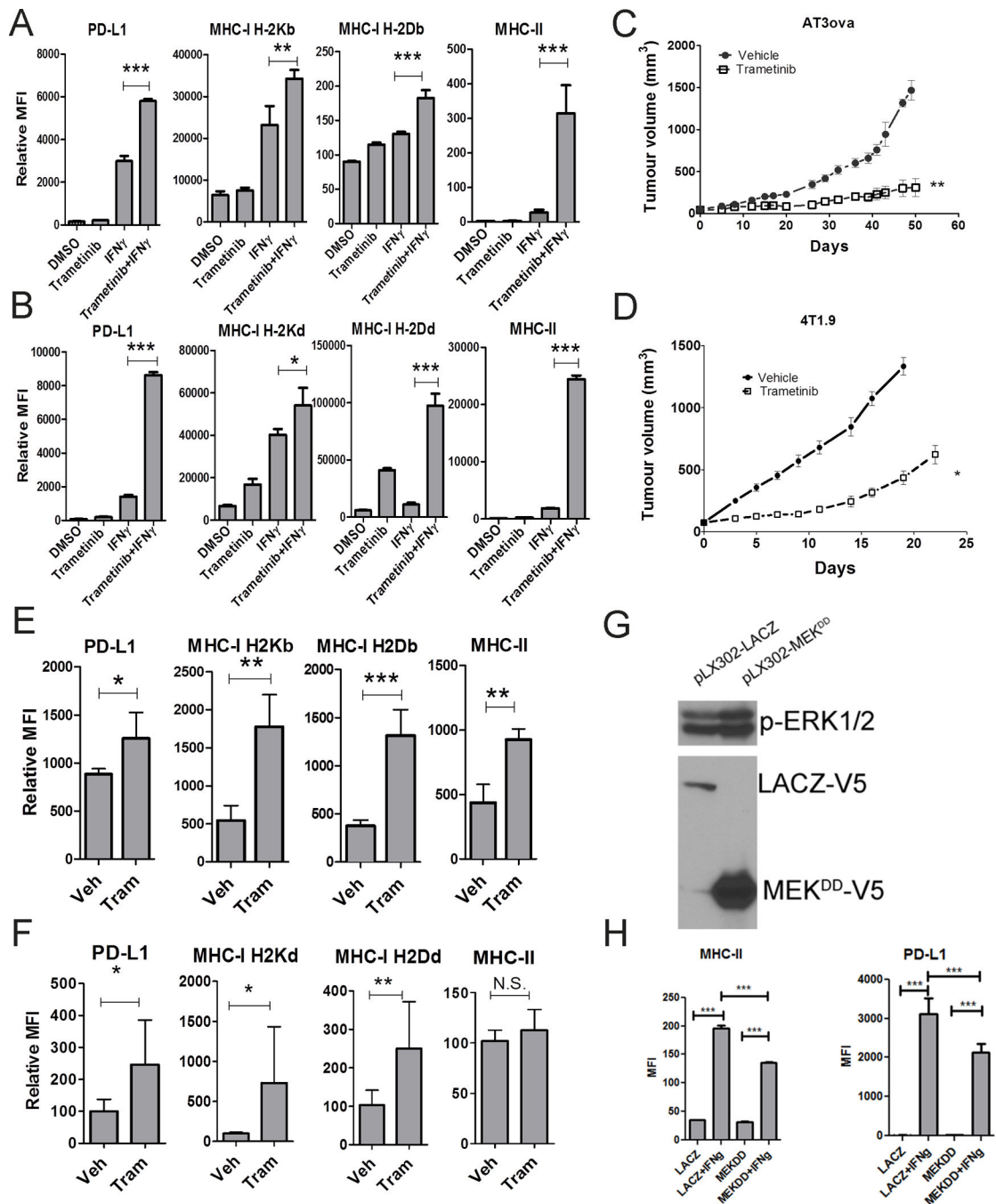


Figure 3. MEK inhibition modulates MHC-I/II and PD-L1 expression in breast cancer models in vitro and in vivo

Flow cytometry analysis of PD-L1, MHC-I and MHC-II expression in the AT3ova (A) and 4T1.9 (B) cell lines after 5 days of treatment with trametinib (100nM) ± IFN γ (100pM) *in vitro*. Data is represented as the mean \pm SD of triplicate samples. At least 2 replicate experiments were performed for both cell lines. P-values represent Tukey's post-hoc test for individual comparisons, upon significant ANOVA. C) and D) AT3ova tumors growing in wild type C57BL/6 mice (C) or orthotopic 4T1.9 tumors growing in wild type Balb/c mice

(D) were treated with trametinib (1mg/kg/daily) or vehicle control for up to 50 days. Tumor volumes were measured 2–3 times weekly. P-values represent result of a repeated-measures ANOVA. E) and F) Tumors from AT3ova and 4T1.9, respectively were subjected to *ex vivo* FACS analysis after 5 days of treatment to determine PD-L1, MHC I and MHC II expression on tumor cells. Data is expressed as mean fluorescence intensity relative to vehicle control tumors and represents n= 6–10 mice per group. P-values represent unpaired student's t-tests. G) MMTV-neu cells were transduced with pLX302-LACZ control or pLX302-MEK^{DD}, a constitutively active mutant, and subjected to western blot to determine MEK activity. H) MMTV-neu-LACZ and MMTV-neu-MEK^{DD} cells were treated with IFN γ for 3 days prior to flow cytometry analysis for PD-L1 and MHC-II. Bars represent mean \pm sd of 3 experiments. P-values represent results of a one-way ANOVA followed by Tukey's post-hoc test. For all panels, * P<0.05; **P<0.01; ***P<0.001.

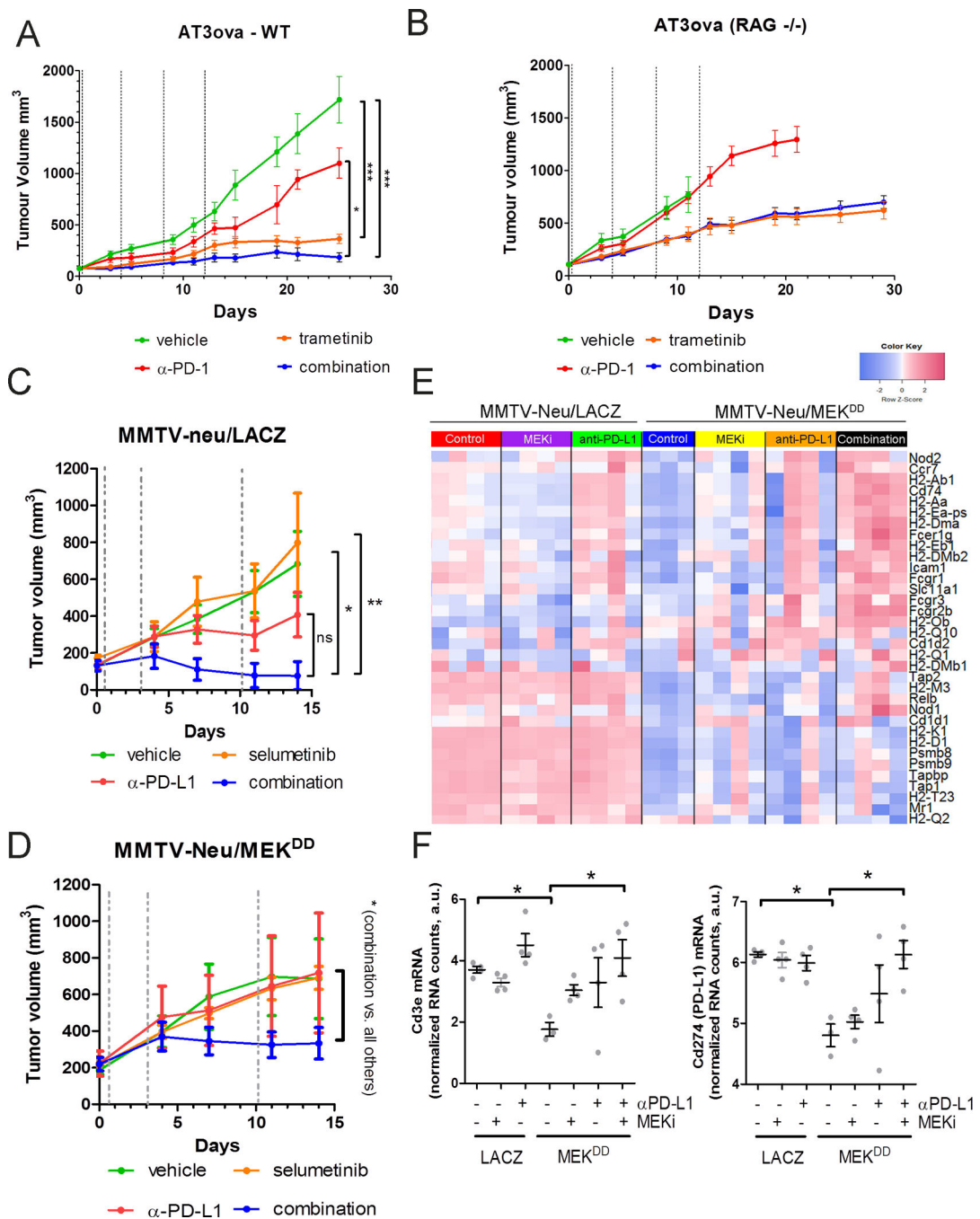


Figure 4. MEK inhibition augments activity of α-PD-1/PD-L1 immunotherapy

A) (left) AT3ova tumors growing in wild type C57BL/6 mice were treated with a vehicle or trametinib at 1mg/kg orally once a day for 30 days and either isotype control antibody injection or α-PD-1 antibody at 200 μg/mouse (days 0, 4, 8 and 12). P-values represent one-way repeated measures ANOVA, with post-hoc Tukey’s test to compare arms. *p<0.05 for each comparison of trametinib + α-PD-1 vs. all others arms. B) Identical experiment to (A) except that the tumors were grown in RAG-deficient mice, lacking a functional immune system. C–D) Orthotopic MMTV-neu tumors (pLX302-LACZ [D] or pLX302-MEK^{DD}[D])

growing in wildtype FVB mice were treated with selumetinib (50mg/kg twice daily) by oral gavage, or α -PD-L1 at 100 μ g/mouse (days 0, 3, and 10). P-values represent one-way repeated measures ANOVA, with post-hoc Tukey's test to compare arms. For (C) * $p < 0.05$ for combination vs. vehicle control and ** $P < 0.01$ for combination vs. selumetinib. For (D), * $P < 0.05$ for each comparison of combination vs. all other arms. E) nanoString analysis (mRNA expression) of tumor cross-sections from study mice from (C–D) for known genes associated with antigen-presentation and processing. Replicate tumors ($n = 3–5$) were analyzed for each treatment group. Combination-treated MMTV-neu/LACZ tumors were not analyzed due to the high complete response rate. F) nanoString gene expression analysis for *Cd3e* and PD-L1 (*Cd274*) in tumors from (C–D). * $p < 0.05$ for multiple-comparisons-corrected Tukey's post-hoc test, utilized post-significant ANOVA.